"Design and Optimization of a Hybrid Air Conditioning System with Thermal Energy Storage Using Phase Change Material"

Ahmed Aljehani[1,2], Siddique Ali K. Razack[3], Ludwig Nitsche[1], Said Al-Hallaj[1, 3, *]

[1] Department of Chemical Engineering, University of Illinois at Chicago, USA
[2] Department of Chemical Engineering, University of Jeddah, Saudi Arabia
[3]AllCell Technologies, LLC. Chicago, USA

*Corresponding author.
Tel.: +1-872-281-7606; fax: +1-773-940-1123
Email: sah@uic.edu

Abstract

This paper evaluates the use of a phase change composite (PCC) material consisting of paraffin wax (n-Tetradecane) and expanded graphite as a potential storage medium for cold thermal energy storage (TES) systems to support air conditioning applications. The PCC-TES system is proposed to be integrated with the vapor compression refrigeration cycle of an air conditioning (AC) system. The use of this PCC material is novel because of its unique material and thermal characteristics as compared to ice or chilled water that are predominantly used in commercial TES systems for air cooling applications. The work of this paper proposed and tested a hypothesis, which suggests that integrating a conventional AC with a PCC-TES would result in significant benefits concerning compressor size, compressor efficiency, electricity consumed and CO_2 emissions. The proposed integration would also contribute to reduce electricity demand during peak hours and reduce necessity to build more expensive power plants and distribution lines. To test the hypothesis, a simulation model in Aspen Plus® software was prepared. However, Aspen Plus® does not have a built-in library to predict PCC's melting and solidification behaviors. Therefore, an analytical heat transfer model was written as a system of equations in Fortran code into Aspen Plus® calculation block to simulate the phase change behavior and associated characteristics. The overall simulation model, which was designed specifically for this research work, consists of two main parts that communicate with each other. The first part simulates the AC's refrigeration loop using the built-in Aspen Plus® components and the second part implements the PCC heat transfer model written within the calculation block of Aspen Plus®. The simulation model was validated by crosschecking the calculated results with actual experimental data from an actual 4 kWh PCC-TES benchtop thermal storage system. Very good agreement was observed between the simulations and laboratory data. Simulated performance of the proposed integration between the AC and the PCC-TES indicated the potential to (1) downsize the compressor by 50%, (2) lower electrical consumption by the compressor by 30%, (3) lower CO_2 emissions by 30%, and (4) double the compressor efficiency during off and mid peak hours. The present work is a conceptual design and optimization study and does not account for integration inefficiencies, energy losses, real-world operation complexity, and added capital cost of TES integration with AC systems.

Keyword: Electricity's Demand Side Management; Air Conditioning; Thermal Energy Storage; Latent Heat Storage; Phase Change Material

LIST OF ABBREVIATIONS

$A_{(eff\text{-}tube)}$	Effective area of heat transfer fluid (HTF)'s tubes
AC	Air Conditioning
A_{PCM}	Surface area of the phase change material (PCM)
COP	Coefficient of Performance
C_p	Specific heat of the phase change material (PCM)
Cp_{eff}	Effective specific heat of the phase change material
d_i	Inside diameter of the heat transfer fluid (HTF) tube
d_o	Outside diameter of the heat transfer fluid (HTF) tube
EG	Ethylene Glycol
h_{fluid}	Heat transfer coefficient of the heat transfer fluid (HTF)
ΔH	Latent heat or Energy content of the PCM per mass
Δh	Energy content per volume of the PCM
m	Mass of the phase change material (PCM)
Δm	Fraction melted (or solidified) of the phase change material (PCM) during phase change
PCC	Phase change composite
PCM	Phase change material
ρ	Density
Q	Cumulative heat or thermal energy
s	Depth or (location) of moving phase boundary
t	Melting duration of the PCM (in units of time)
TES	Thermal energy storage
T_f	Final temperature of the PCM
T_i	Initial temperature of the PCM
T_m	Melting temperature of the PCM
λ_{PCM}	Thermal conductivity of the PCM
λ_{wall}	Thermal conductivity of the heat transfer fluid (HTF) tube wall

1. Introduction, Motivation and Hypothesis

A large portion of electricity consumptions in the US and all over the world is associated with air conditioners especially during summer seasons. According to the US Department of Energy, air conditioners annually cost homeowners around 29 billion dollars and release 117 million tons of CO_2 to the air [1]. A recent study [2] revealed that approximately one fifth of the electricity consumption in Austin Texas during peak hours is attributed to air conditioners operated in single-family residential homes. A similar study conducted in Spain revealed that air conditioners are responsible of more than one third of the electricity consumption during peak hours in Madrid [3]. Likewise, a study of Saudi Arabia's electricity consumption [4] revealed that air conditioners account for 50% of the increase in peak demand during summer months. The air conditioner (AC) units in the US and around the world are mostly oversized to meet peak cooling load during hot summer days. The underutilized capacity of oversized AC units wastes a significant amount electricity during cooler hours/days of the year and increases carbon emissions. Moreover, high demand of electricity during peak hours drives up the transient price of electricity. In the US, for example, Southern California Edison Electric utility company applies time of usage (ToU) electricity charges during peak hours which is 0.235 $/kWh from 12 pm to 6 pm plus a demand charge of $9.5/MAX kW for each billing cycle [5]. The company applies $0.191/kWh and $0.064/kWh electricity ToU charges for mid-peak and off-peak hours, respectively. Furthermore, at some parts of the world, high electricity demand at once during peak hours may even lead to power outages.

On the production side, utility companies are adopting various energy efficiency programs and energy storage technologies to offset carbon emissions and avoid building new additional power plants and distribution lines to meet the peak electricity demands. On the demand side, residential and commercial customers are motivated to avoid ToU electricity charges and demand charges by opting for alternative technologies that are available or emerging in the market. A thermal energy storage (TES) system is a good alternative solution for demand-side management to shift the AC electricity usage from peak hours to off-peak hours, thereby also reducing the overall carbon footprint compared to a conventional air conditioning system.

A typical TES system cools the building during peak hours (when electricity prices are high) by absorbing heat from the incoming hot air for the spaces that need to be cooled. At night (when electricity prices are low), the TES then rejects the stored heat by exchange with the refrigeration loop of a conventional AC. The TES system will be integrated with an AC unit such that the TES system can provide additional cooling to the building during peak hours by completely or partially shifting the cooling load.

The concept of integrating cold thermal energy storage (TES) into an air conditioning (AC) system has been widely evaluated in the literature aiming to partially or completely shift electricity demand from peak hours to off-peak hours [6–12]. TES systems integrated with AC can be generally classified into groups; sensible heat versus latent heat. A sensible heat storage system utilizes liquid or solids to store energy on the basis of heat capacity over a range of temperatures. A latent heat TES system, on the other hand, stores energy at the temperature of (or within a narrow band of temperatures covering) a phase transition, either solid-liquid or solid-solid. Both cases have been described by phase change materials (PCM), although henceforth in our application we shall mean solid-liquid. Latent heat is much larger than sensible heat, so latent heat systems are typically more compact.

As examples of latent heat versus sensible heat systems, respectively, ice and chilled water have been popularly used for commercial cold (TES) applications integrated into a conventional air conditioning system [9–12]. However, ice-TES systems also have some disadvantages such as super cooling issues, low thermal conductivity and low melting temperature [13]. Thus, they need to be oversized to accommodate more of the (highly conductive) tubes to speed up the thermal response. Alternately, the vapor compression refrigeration loop can be upsized to speed up solidification within the limited night hours. But this partially negates the purpose of integrating TES and reduces overall operating efficiency of the ice-TES by 30% - 40% [13]. Clearly, neither oversizing refrigeration loop that cools the ice-TES system nor using extremely large number of highly conductive tubes is a cost effective solution. Chilled water TES, on the other hand, is a very mature system to divert electricity consumption from day to night [11]. Given the relatively low thermal capacity of sensible heat (compered to latent heat), chilled water systems need very large equipment sizing to operate efficiently [11]. They are only economical for very large loads – typically 7,000 kWh or higher [12].

In light of the aforementioned deficiencies with ice and chilled water TES systems, a wide variety of PCMs evaluated in the literature [6,7,14] possess certain strengths and weaknesses depending on the intended application. However, only few of those evaluated PCMs are feasible candidates for cold latent heat TES storages. For commercial rooftop air conditioning applications, the optimum melting temperature of a PCM should be in the range of 5-9 ^{o}C and the latent heat and thermal conductivities should be relatively high. PCMs also need to be chemically stable, uniform during melting/solidification (i.e., producing no phase segregation), non-toxic, non-corrosive, and readily available at low cost [6,7,14]. Among the paraffin family, n-Tetradcane ($C_{14}H_{30}$) and n-Hexadecane ($C_{16}H_{34}$) are the most appropriate paraffin waxes for cold storage applications. $C_{14}H_{30}$ alkane has a melting temperature of 5.8 ^{o}C and a theoretical latent heat value of 227 kJ/kg, while n-hexadecane has a higher

latent heat value (236 kJ/kg) and a higher melting point of 18.1 °C [7]. The melting point of n-tetradcane ($C_{14}H_{30}$) lies within the advantageous range of 5-9 °C, making it the more suitable choice for a cold TES application.

Composite microstructure can significantly enhance the properties of thermal conductivity and/or uniformity. Such materials are called phase change composite (PCC) materials or composite phase change (CPC) materials; we shall employ the former term. Our research utilized a PCC material consisting of about 78% low temperature paraffin (alkane) and 22% expanded graphite. The paraffin is described by [14] *as "saturated hydrocarbon mixtures and normally consist of a mixture of mostly straight chain n-alkanes, CH3–(CH2)n–CH3".* The paraffin has several advantages: chemical stability, tunable melting point/range based upon composition, uniform melting/solidification (producing no phase segregation), and also absence of toxicity, corrosivity and super cooling issues [6,7,14]. However, the paraffin has lower thermal conductivity. Many researches have tried to improve thermal conductivity of paraffin waxes with various additives such as alumina (Al_2O_3) [15], but these additives provide small improvement. The proposed PCC material described in this paper can achieve a thermal conductivity of approximately 22 W/m-K (approximately ten times the thermal conductivity of ice) due to the presence of expanded graphite three-dimensional structure as discussed in the literature [16].

This paper evaluates the effectiveness of a PCC material (consisting of n-Tetradecane paraffin wax and expanded graphite) as the storage medium for a TES system integrated into AC as a demand side management solution. We test the following hypothesis:

> <u>Hypothesis.</u> *Integrating the vapor compression refrigeration cycle of a conventional AC with a PCC-TES as a demand side management solution would provide significant benefits for electrical consumption and demand side management. The proposed [AC + PCC-TES] integration would (1) reduce the refrigeration compressor size requirement (and thereby attendant power consumption, CO_2 emissions, and capital costs), and (2) enhance efficiency in all modes of operation: off-peak, mid peak and peak. The aggregate effect of these advantages could ultimately reduce necessity to build more expensive power plants and distribution lines.*

To test the hypothesis, a computer model of the proposed [AC + PCC-TES] system was developed using Aspen Plus® process simulation software. Since Aspen Plus® does not have a built-in library to predict the melting and solidification behaviors of PCC, we formulated a suitable mathematical heat transfer model as a system of equations and programmed their solution in Fortran. This represented phase-change behavior

and associated thermodynamic and transport properties and was implemented using a Calculator Block residing within and communicating with the larger Aspen Plus® model. The simulations were validated using actual experimental data from a 4 kWh PCC-TES benchtop thermal storage system. Simulated parametric study then furnished quantitative scenarios and our estimates of the gains expected with [AC + PCC-TES].

2. Proposed System and Research Approach

To guide formulation of the overall theoretical/computational model, and specifically of the block diagram in Aspen Plus®, we first address the [AC + PCC-TES] approach with reference to conceptual flowsheets that illustrate the complete system and its operation in charging (night) versus discharging (peak day) modes. As our point of departure, Figure 1 depicts a conventional AC refrigeration cycle where all of the air cooling occurs within the evaporator. Figure 2a illustrates one possible integration of AC with PCC-TES. In discharging mode (Figure 2b) during peak daytime hours, a portion of the incoming hot air stream is rerouted from the evaporator (air handling unit) to the hot air/EG exchanger where EG Loop #1 mediates cooling with the PCC material. Lifting a portion of the peak cooling load from the AC cycle (partial shaving) means that the compressor can be reduced in size. An alternative approach would be to completely shave the cooling load during peak hours by designing a larger PCC-TES system to entirely cool the hot air stream without operating the AC cycle at all. c illustrates the charging mode, at which the PCC-TES rejects the stored heat and solidifies utilizing the vapor compression refrigeration loop of the conventional AC during inexpensive off-peakoff-peak hours.

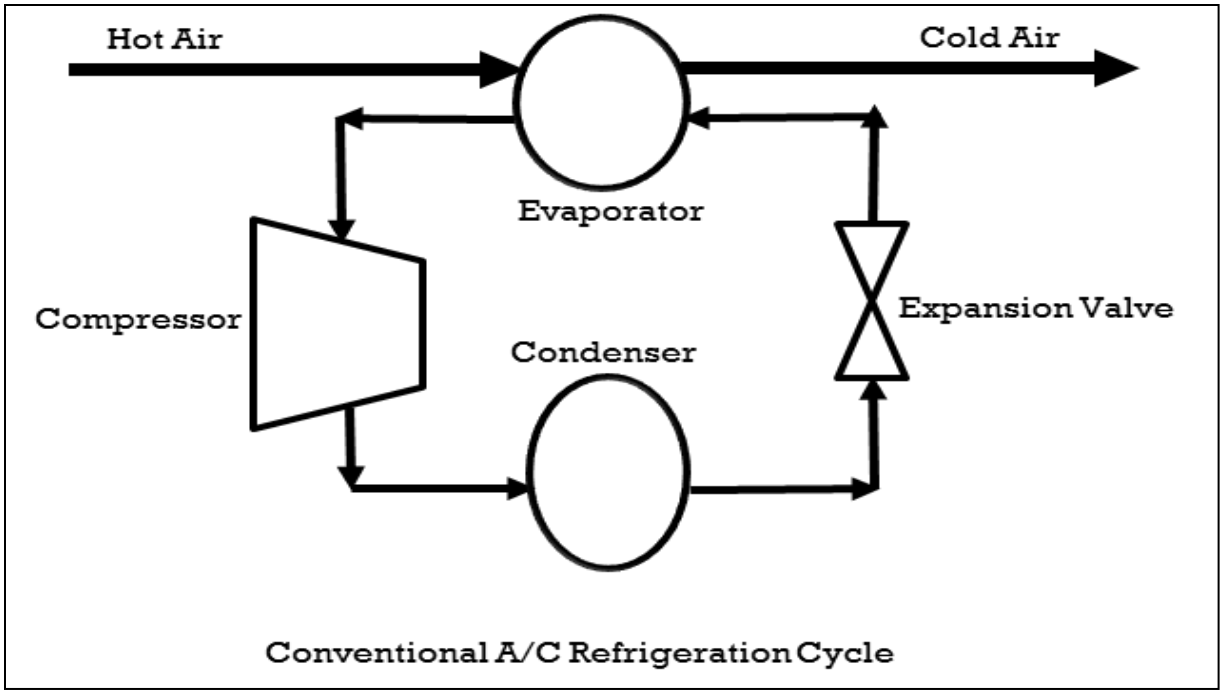

Figure 1: AC's conventional refrigeration cycle

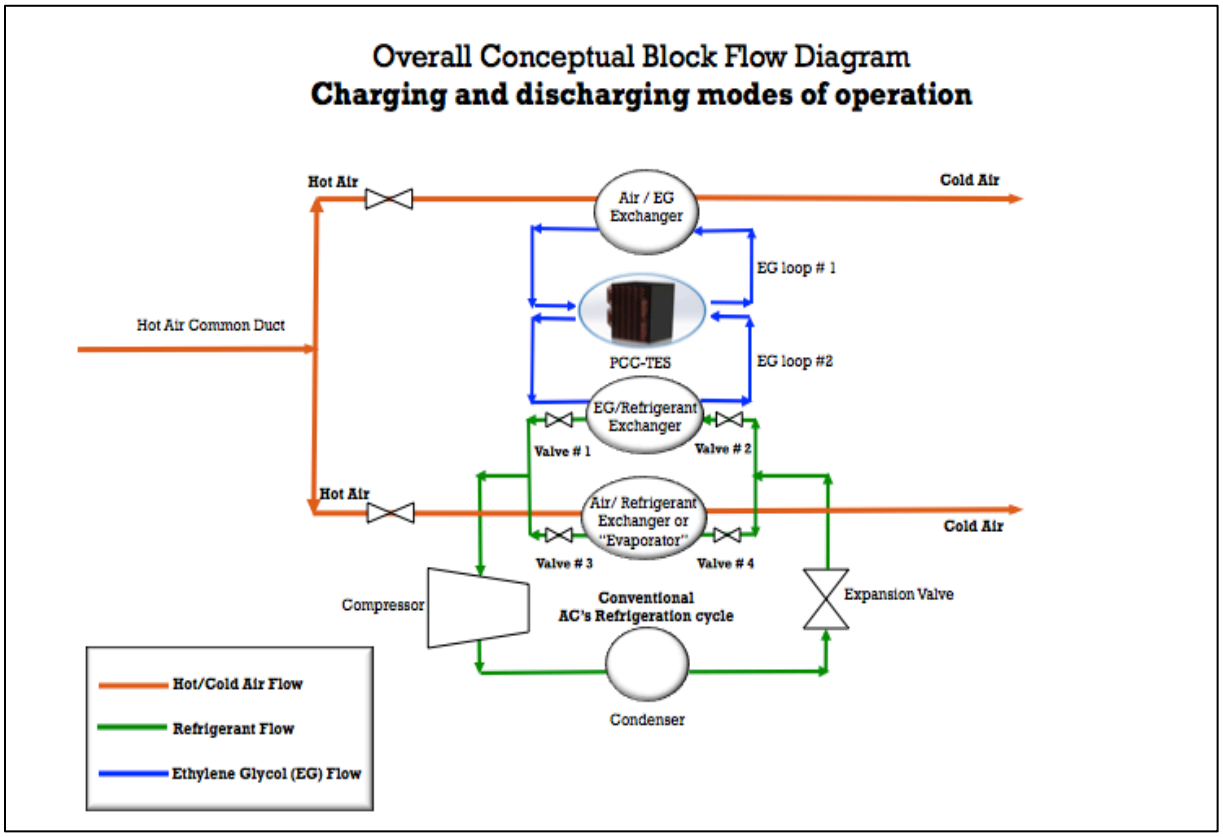

Figure 2a: Complete system. EG Loop #1 mediates heat exchange between incoming hot air and the (thawing) PCC during discharging mode. EG Loop #2 mediates heat exchange between the refrigerant and the (freezing) PCC during charging mode.

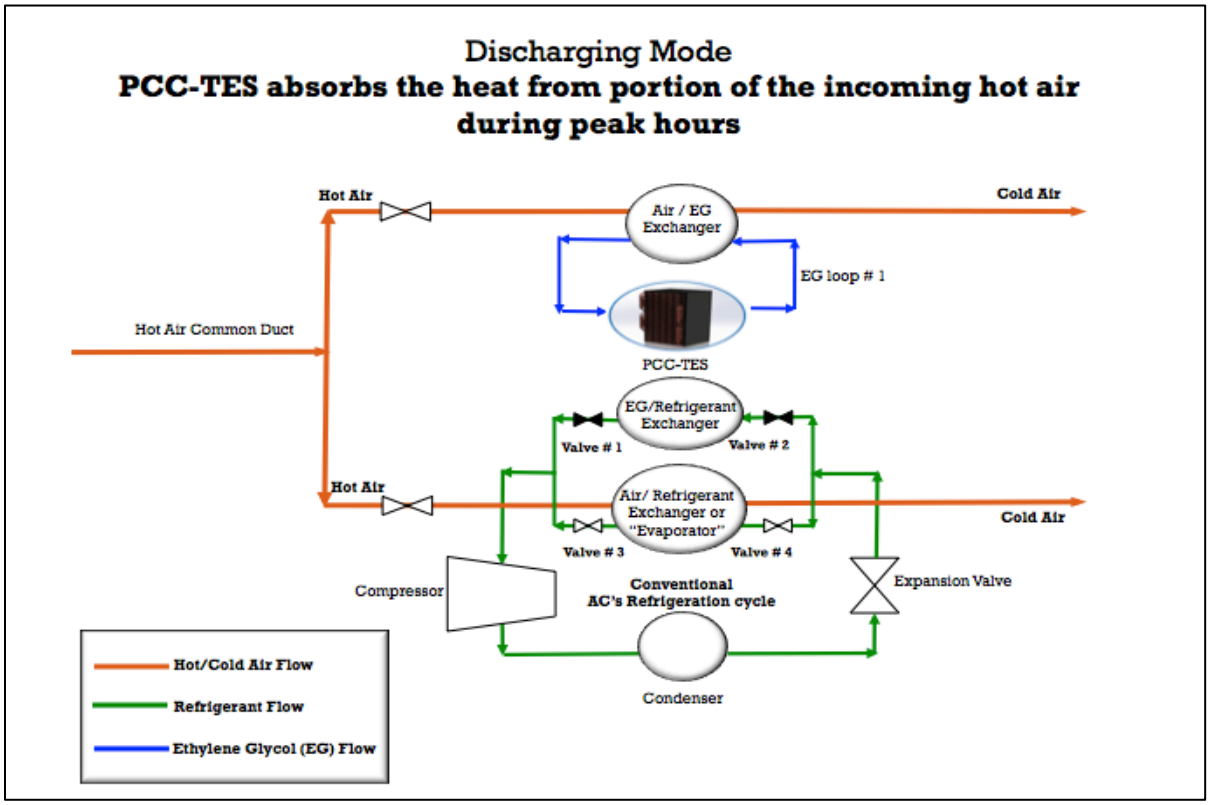

Figure 2b: Discharging mode operates with valves 1 and 2 closed and valves 3 and 4 open. During peak day hours cooling of hot air is divided between the refrigerant loop and the melting PCC.

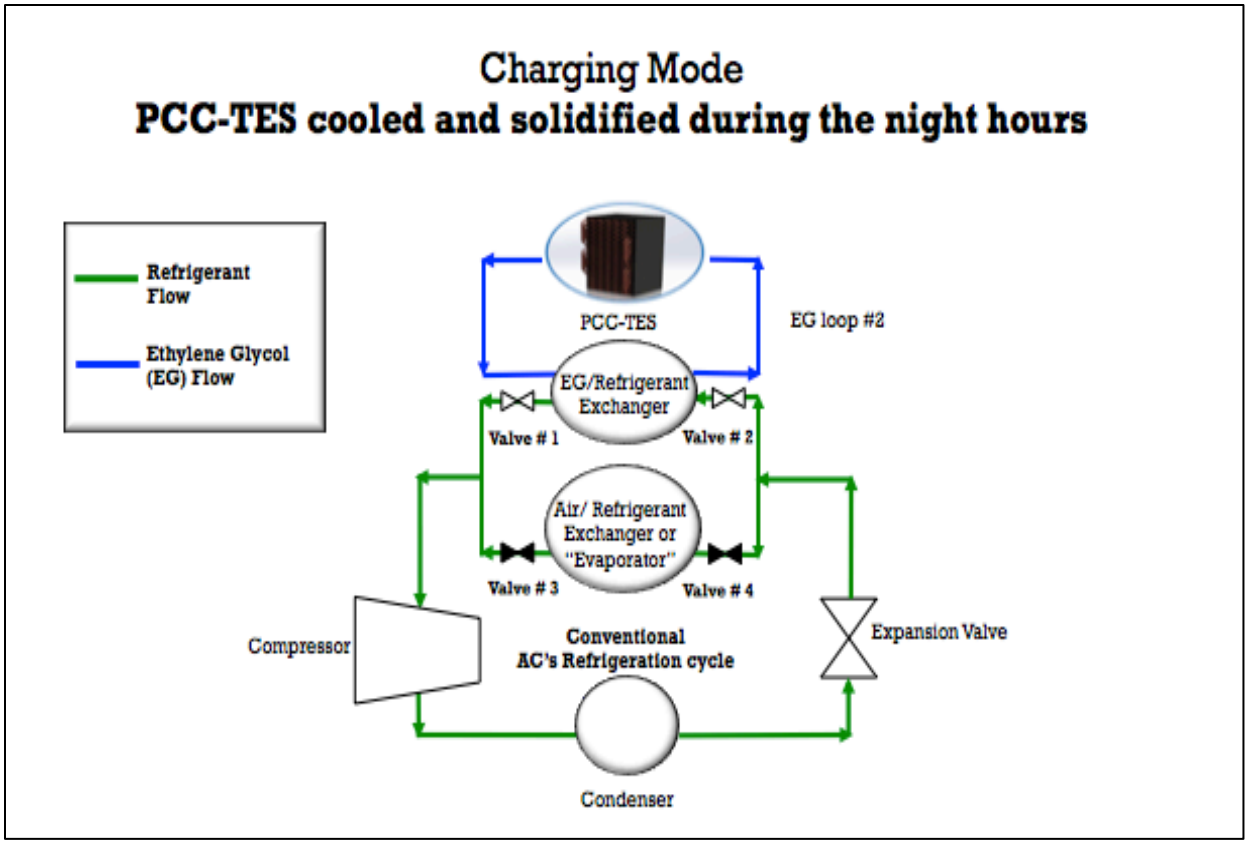

Figure 2c: Charging mode operates with valves 1 and 2 open and valves 3 and 4 closed. During night hours the AC refrigerant loop cools and freezes the PCC.

The PCC-TES system (Figures 3a and 3b) consists of a stack of 28 slabs of PCC material that is composed of graphite and low temperature phase change material (PCM). Each slab is W x D x H mm and weighs x.x kg (22% graphite and 78% graphite). Graphite is the structure that holds the phase change material PCM, which is straight chain paraffin (n-Tetradecane or $C_{14}H_{30}$), and boosts the overall thermal conductivity of the composite. The paraffin, n-Tetradecane ($C_{14}H_{30}$), serves as the PCM that is capable of storing or releasing a large amount of heat during the phase change (solid to liquid) or (liquid to solid). The whole PCC-TES structure is thermally insulated with building insulation materials. Each slab is a graphite structure that has been pressed and then soaked into a bath of n-Tetradecane for at least 24 hours until impregnated with n-Tetradecane. The slabs are numbered from top to bottom; top being number 1. As illustrated in (Figures 3a and 3b), copper tubes pass back and forth in between the 28 slabs. A stream of Ethylene Glycol (EG) runs through the copper tubes. EG enters the PCC-TES structure at the top and exit from the bottom of the structure. EG (as illustrated by Figure 2a, loop # 1) mediates heat exchange between incoming hot air and the (thawing) PCC during discharging mode.

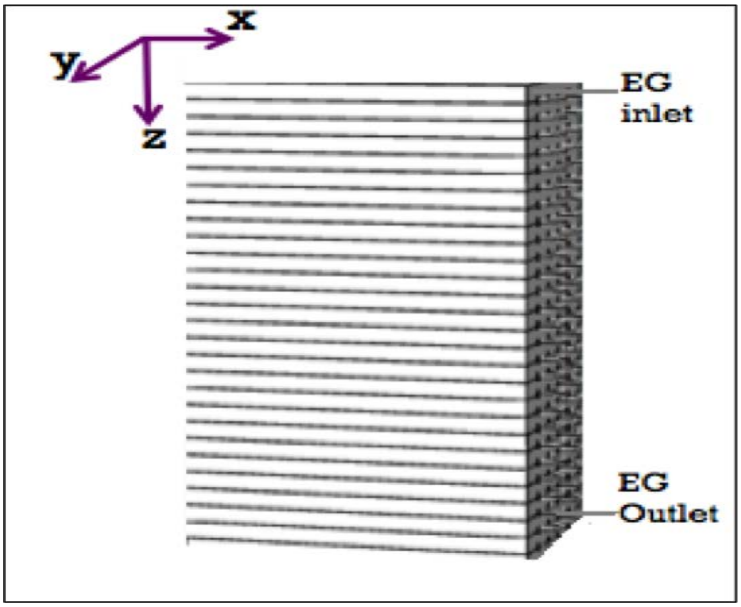

Figure 3a: PCC-TES conceptual design; PCC-TES exchanging heat with EG stream

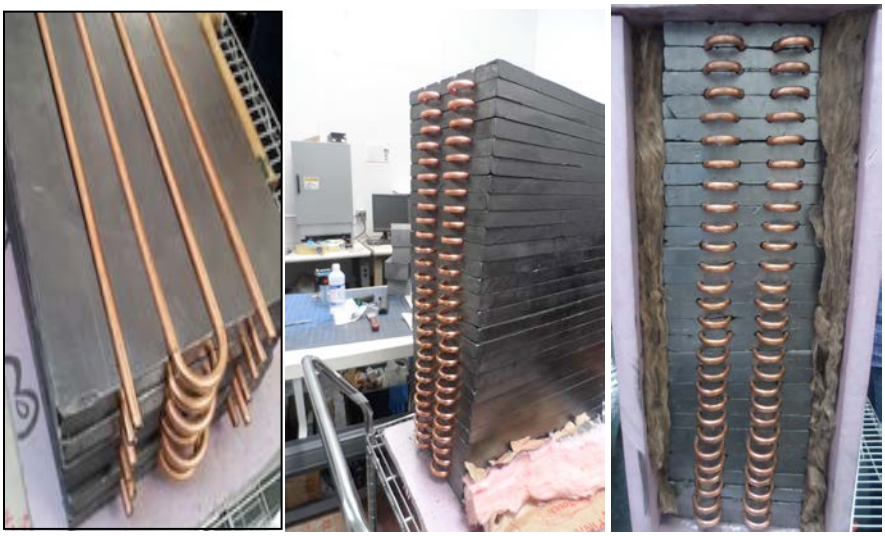

Figure 3b: Actual representation of the proposed PCC-TES system

2.1 The Aspen Plus® model

Guided by the conceptual flowsheet, the first part of the simulation model was built with the Aspen Plus® flowsheet environment imitating the overall integration between the PCC-TES and the AC system. This portion simulates the AC's vapor compression refrigeration loop, both EG loops and the hot and cold air streams

entering and exiting the air-handling units. Although Aspen Plus® can suitably simulate an air conditioning's refrigeration loop, it does not have a built-in library to predict melting and solidification behaviors of a PCC material. The accurate computation of melting and solidification behavior would assist in estimating the heat absorbed/released in association with any particular stage of melting or solidification, respectively. This section will give some light about the generation of the Aspen Plus® flowsheets while the next section will address the mathematical heat transfer model that we formulated as a system of equations and programmed it into Fortran; which was eventually written within a calculation block in Aspen Plus® to communicate with the Aspen Plus® simulation environment.

Three Aspen Plus® main flowsheets were generated. The first flowsheet simulates a conventional vapor compression refrigeration loop of a conventional air conditioning system. This supplies either (1) the entire cooling load (base case) or (2) half of the cooling load (reduced load case), being augmented by the PCC-TES. The second flowsheet simulates the discharging mode of the PCC-TES, by which PCC-TES meets the remaining half of the cooling demand by melting the PCC material. Even though the AC and the PCC-TES work jointly (in the proposed integration scenario) to meet the cooling demand, the two systems were simulated in two different flowsheets to avoid confusion and to show that each process is independently meeting half of the entire cooling demand on its own. The third flowsheet simulates the charging mode of the PCC-TES; at which the conventional vapor compression refrigeration loop will cool and solidify the PCC-TES during the night. Even though the AC and the PCC-TES work jointly to meet the cooling demand requirement, the two systems were simulated to show that each process is independently meeting half of the entire cooling demand on its own.

The development of the flowsheets was associated with two main challenges:

The first challenge was the fact that Aspen Plus® does not have a built-in library to predict the melting and solidification behaviors of PCC and associated thermodynamics and transport properties. Therefore, to overcome the first challenge, we formulated a suitable mathematical heat transfer model as a system of equations and programmed their solution in Fortran. This represented phase-change behavior and associated thermodynamic and transport properties and was implemented using a Calculator Block residing within and communicating with the larger Aspen Plus® model. With that, the calculator block of Aspen Plus® is now acknowledging the fact that the PCC-TES is melting while cooling the EG stream that is cooling the air. Depending on the heat content, initial and final temperatures of the PCC-TES and all other necessary data (such as mass flow and initial temperatures of air and EG streams.etc), Aspen Plus® now can estimate the energy absorbed by the PCC-TES and

the melted PCC fraction and make necessary calculations to estimate the steady state temperatures of the EG and air streams.

The second challenge was the fact that we were interested in melting duration, while Aspen Plus® would land into the overall steady state solution of the overall system. We were not only interested in the EG steady state temperature during the PCC-TES phase change duration, the total energy absorbed by the PCC-TES and melted fraction, but also, interested in the position of the melting front in z-dimension (top to bottom) and the melting duration of each segment within the overall 28-slabs stack. The PCC-TES is gradually melting from top to bottom in association with the hot EG stream circulating and passing through the PCC-TES stack from the top to bottom. So, to overcome this challenge, we employed the "Sensitivity Analysis" feature within Aspen Plus® to calculate melting duration. The formulated mathematical heat transfer model was also utilized within the "Sensitivity Analysis" feature to describe the melting progression. The "Sensitivity Analysis" now provides an estimate of heat absorbed by one segment at that particular quasi steady state along with estimates of the position of the melting front in z-dimension (in length units) and the time duration that would take a particular segment to melt. The theory, scientific equations and consequently the mathematical model will be discussed in detail in the next section of this paper.

3. Theoretical background and foundations

As briefly introduced in the previous section, the second part of the simulation model is the mathematical representation of melting and solidification behaviors within the PCC material. This requires modeling the position and movement of the moving phase boundary between the liquid and solid phases within the PCC material. The resulting system of equations is implemented in a Fortran code within the calculation block of Aspen Plus®. This block exchanges data with the Aspen Plus® simulation environment.

In one space dimension the moving boundary surface is described by the classic Stefan problem; which is a well-recognized scientific research work concerning solid-liquid phase changes performed by J Stefan and published between the years of 1889 to 1891[17–19]. The history of the well scientifically recognized classic Stefan problem is described by [18] "*In 1889 Stefan had written four papers on free boundary problems. The paper on ice formation in the polar seas was reprinted in 1891 and has drawn the most attention of the scientific community*". As described by [17,18] the classic Stefan problem evaluated by Stefan [1891] studied the freezing behavior of a seawater quantity, a material that may exit in solid or liquid phases. The seawater is initially at liquid state. The temperature of the air adjacent to the surface of the seawater is

dropped to a temperature below the freezing temperature of the seawater. Accordingly, a solid layer of seawater is formed at the interface between air and seawater. The solid layer formed grows with time. Stefan calculated the thickness (h) of the solid layer within time (t). Stefan assumed a linear temperature within the ice in view of the fact that specific heat of ice is much smaller than latent heat.

The work presented in this work, just like the classic Stefan problem, illustrates an external heat source is being applied to the surface of the phase change material causing a phase change from solid to liquid or liquid to solid while absorbing or rejecting heat, respectively depending on the temperature of the heat source and the characteristic melting/solidification temperature of the phase change material. A moving boundary surface during the solid to liquid phase transition (or vice versa) is generated between the two states of the matter. As illustrated in the literature[20], "the continuously moving phase change boundary has to be tracked accurately throughout a region approximated by a finite number of points".

It is worth mentioning that the heat transfer problem addressed in this present work is different than the classic Stefan problem. In particular, the external heat source is actually distributed within the phase change material volume not introduced to the outside surface of the material. Therefore, the work introduced later on 2003 by Kostenko et al [21] addressed the case where the external heat source was not on the outside surface of the phase change material volumetric structure, but it was actually distributed within the volume and stated *"we claim that the celebrated Stefan condition on the moving interphase, accepted in mathematical physics, can not be imposed if energy sources are spatially distributed in the volume. A method based on Tikhonov and Samarskii ideas for numerical solution of the problem is developed."* As discussed by Kostenko et al [21], the classic Stefan problem had the two conditions (1) & (2) as follow:

$$K_{sol}\frac{\partial T\,(xs+0,t)}{\partial x} - K_{liq}\frac{\partial T\,(xs-0,t)}{\partial x} = L\rho_{sol}V_s$$ Condition (1) *; reference* [21]

$$T|s = T^*$$ Condition (2) ; *reference* [21]

Where, in condition (1) as discussed by Kostenko et al [21], left hand side of the equation describe the heat flux per area over time in accordance with Fourier law. Heat flux is proportional to temperature gradient and material thermal conductivity. Right side of condition (1), as discussed Kostenko et al [21] takes into account latent heat and density of phase change material in addition to velocity of moving boundary. Condition (2), as discussed by Kostenko et al [21] illustrates temperature continuity where temperature at the surface, between the two phases of solid and liquid, equals

the temperature of the phase transition. Kostenko et al [21] discussed that the external heat source is not distributed within the volume therefore q(x,t) is eliminated in the conservation of energy equation presented by the classical Stefan problem.

Furthermore, as illustrated by Kostenko et al [21], the method by [*Tikhonov and Samarskii*] formulated the conservation of energy equation illustrated by Equation (3). Where, L δ(T – T*) ∂T/∂t and ρC ∂T/∂t represent the heat added because of the phase transformation (latent heat of fusion) and the sensible heat stored, respectively. L is the latent heat of fusion, C is the specific heat and ρ is the density. On the other hand, v grad T represents the heat transported due to convection of molten material.

$(\rho C + L\ \delta\ (T - T^*))\ (\frac{\partial T}{\partial t} + v\ grad\ T) = div\ (K\ grad\ T) + q\ (x, t)$ *(3); reference* [21]

The work by Kostenko et al [21] proved that Equation (3) may provide a better description of the case where the external heat is distributed within the phase change material's volume at which conditions (1) and (2) are not applicable. Furthermore, Kostenko et al [21] ignored the heat transported due to convection of molten material (illustrated by v grad T) to simplify the problem. Moreover, Kostenko et al [21] assumed flux uniformity in the x-direction. Therefore, the term q(x, t) became q(t) and the (K grad T) term is dropped. So Equation (3) become Equation (4) according to the method formulated by Kostenko et al:

$(\rho C + L\ \delta\ (T - T^*))\ (\frac{\partial T}{\partial t}) = q\ (t)$ (4) *; reference* [21]

Equation 4 in simple words is equating the heat absorbed, because of the phase transformation (latent heat of fusion) and the sensible heat stored, with the heat rejected from the heat source. Another way to describe Equation (4) will be Equation (4a) and employing the effective specific heat method, as follow:

$$[\rho\ V\ Cp_{eff}]\ \frac{\partial T}{\partial t} = q(t) \qquad (4a)$$

Where ρ is the density and V is the volume of the phase change material.

Cp_{eff} is the effective specific heat of the phase change material; which can be defined along the temperature profile with the Equations (4b-4e) with reference to [22]:

$Cp_{eff} = Cp_s$, $\quad if \quad T < T_s$ (4b)*; reference* [22]

$Cp_{eff} = Cp_s + \frac{\Delta H\ (T - T_s)}{(T_m - T_s)^2}$, $\quad if \quad T_s \leq T \leq T_m$ (4c)*; reference,* [22]

$$Cp_{eff} = Cp_s + \frac{\Delta H\ (2T_m - T - T_s)}{(T_m - T_s)^2}, \quad if \quad T_m < T \leq T_l \qquad (4d);\ reference,\ [22]$$

$$Cp_{eff} = Cp_l, \quad if \quad T > T_l \qquad (4e);\ reference,\ [22]$$

Where, Cp_s is the specific heat for the phase change material at solid phase, Cp_l is the specific heat for the phase change material at liquid phase, ΔH is the latent heat of the phase change material or in other words the energy content per mass of the phase change material, T_s is the temperature at which (and below which) the PCC material is completely solid. T_l is the temperature at which (and above which) the PCC material is completely liquid. T_m is a middle temperature between T_s and T_l during the phase change. ΔH represents the latent heat of the PCC during the phase change.

Similarly, in this present work, the entire PCC-TES can be considered as the heat sink (one finite volume) while the heat transfer fluid (Ethylene glycol) would be treated as the distributed heat source as addressed by Kostenko et al. Therefore, we are interested in describing the overall behavior of the entire PCC-TES system from top to bottom. It is worth mentioning that, the magnitude of heat released by the hot EG is certainly proportional to the effective surface area of the copper tubes. Therefore, the effective surface area of the copper tubes passing through the PCC-TES structure was calculated. The effective surface area is a function of the surface area of a single tube multiplied by the length of a single tube multiplied by the number of tube passes within the PCC-TES structure. Likewise, the magnitude of heat released by the hot EG is certainly proportional to the heat transfer coefficient of EG. The heat transfer coefficient will be calculated following the calculation of Reynolds and Nusselt numbers. The spatial position (in z-direction) of the boundary surface at the upper surface of the upper most slab of the PCC-TES structure is considered the starting point of the volumetric heat exchange emerged. The position in z-direction at the bottom surface of the bottom most slab of the PCC-TES structure is considered the end point of the volumetric heat exchange emerging. The PCC-TES structure is thermally insulated from all sides. The whole system was discretized using an analytical model to calculate time duration for the melting progression of the overall homogenous structure, from top to bottom, as will be discussed in next section.

4. The analytical model accounting for latent/sensible heat and time duration

The absorption and rejection of thermal energy by a phase change material involves both the latent and sensible heat:

$$Q = \int_{Ti}^{Tf} m\, Cp_{eff}\, dT \qquad (5)$$

Q in Equation (5) is equal to the cumulative heat or thermal energy (absorbed or rejected) by the phase change material, m is the mass of the phase change material (PCM), Cp_{eff} is the effective specific heat of the phase change material; which can be defined along the temperature profile by the Equations (4b-4e) described earlier with reference to [22]. Moreover, T_i and T_f are the initial and final temperatures of the PCM, respectively.

For a single component, such as ice, the melting temperature is a single point at which melting or solidification occurs. However, for a composite of several components, the melting temperature cannot be described by a single point melting temperature, therefore melting temperature for a composite would be represented using a melting range. Recall that the PCC melting temperature range is (4-6 ^{o}C); where 4 ^{o}C marks completely solid temperature and 6 ^{o}C marks completely liquid temperature.

The melting range of a composite phase change material approximated to have a direct relationship with melted or solidified fraction in the process of absorbing or releasing heat, respectively as expressed in Equation (6) with reference to the "Liquid fraction - PCM Temperature relationship" discussed in article [24]:

$$melted\ fraction = \frac{(T - T_s)}{(T_l - T_s)} \qquad (6)$$; reference [24]

Where T is the PCM actual temperature. T_s is the temperature at which (or lower) PCM is completely solid. T_l is the temperature at which (or higher) PCM is completely liquid.

"Liquid fraction- PCM Temperature relationship" was further illustrated by [24]:

- Liquid fraction = 0, if $T < T_s$
- Liquid fraction= between 0 and 1, if $T_s < T < T_l$
- Liquid fraction = 1, if $T > T_l$

4.1 Characterization of melting and solidification behaviors

The heat rejected or absorbed by phase change material is associated with valuable information to researchers and designers such as charging and discharging rates,

fraction melted (or solidified) of the PCM, location of the moving phase boundary between liquid and solid phases in space, and melting duration. Therefore, Equation (5) was used to calculate the sensible/latent heat depend on the temperature and discharging/charging rates. Equation (6) was utilized to calculate the melting fraction. To predict the melting time duration an analytical model discussed by [25] and [26] was utilized in this present work. These models not only can calculate time duration, but also are valuable to study effect of multiple variables on the overall heat transfer process such as PCM thermal conductivity, surface area of the PCM, optimum surface area of tubes and optimum heat transfer fluid characteristics, etc. The analytical model as described by [25] assumed a couple of assumptions to simplify a complicated approach and land into an analytical solution. In this present work assumptions were produced with reference to [25–27] heat transfer model major assumptions:

1. Only latent heat is considered during melting stage.
2. Only sensible heat is considered during the duration of the sensible heat exchange before and after melting.
3. Accordingly, assumed a one-dimensional heat transfer in z-direction in the PCC-TES in corresponds to hot fluid temperature profile that is entering the top of the PCC-TES structure and leaves off the bottom as illustrated by Figures 3a and 3b.
4. Within the PCM, heat is transferred by conduction only. There is no heat transfer by convection since the PCM particles are stationed and trapped within the graphite porous structure.
5. Negligible volume variation between solid and liquid states.
6. Well-insulated system.
7. In discharging (melting mode), PCM is initially completely solid. While, in charging mode (solidifying mode), PCM is initially completely liquid.

According to similar derivation to references [25,26], Equation (7) was generated. Equation (7) calculates the time required for each volumetric segment to melt, with respect to location in space (s) in z-direction and temperature of the PCC, as a result of the distributed hot ethylene glycol passing through the PCC-TES structure. A similar approach was used to calculate the sensible heat's duration before and after melting. For sensible heat duration, only sensible heat was accounted. On this case, latent heat terms were replaced with sensible heat terms.

$$t = \frac{\Delta m * \Delta h \ * s^2}{2 * \lambda_{PCM} * \Delta T} \left(\frac{A_{PCM}}{A_{eff-tube}}\right)\left(1 + \frac{2 * \lambda_{PCM}}{s * k}\right) \quad (7)$$

In Equation (7), t represents the melting duration of the PCM (in units of time), Δm represents the fraction melted (or solidified) of the PCM during phase transition, Δh represents the energy content per volume of PCM, while s represents the depth or (the location of the liquid/solid moving phase boundary of the PCM). $\left(\frac{A_{PCM}}{A_{eff-tube}}\right)$ is the ratio of surface area of PCM to effective surface area of heat transfer fluid's (HTF) tube.

λ_{PCM} is the thermal conductivity of the PCM. T_{pcmf}, & T_{pcmi} are the final and initial temperatures of the PCM, respectively, and $\frac{1}{k}$ is described by Equation (8) as follow:

$$\frac{1}{k} = \left(\frac{d_o - d_i}{\lambda_{wall}} + \frac{1}{h_{fluid}}\right) \qquad (8)$$

Where, h_{fluid} is the heat transfer coefficient of the HTF, d_i and d_o are the inside and outside diameters of the HTF's tube, respectively, and λ_{wall} is thermal conductivity of the HTF's tube wall. It is worth mentioning that the derivation by [25,26] started by first setting the heat absorbed by the PCM equal to the heat released by the heat transfer fluid (HTF) as illustrated. This is a similar approach to Equation (4a) discussed earlier in the theoretical background and foundation section, at which heat absorbed, because of the phase transformation (latent heat of fusion) and the sensible heat stored, is equated with the heat rejected from the heat source. The s(t) in Equation (7) is calculated based on Equation (9).

$$s(t) = \frac{Q}{A * \Delta h} \qquad (9)$$

Where, Q is the heat absorbed in (kJ) by each segment (calculated using Equation 5), A is the surface area of each segment, and Δh is the energy content per volume of the segment. Figure 4 describes the conceptual approach used to discretize the model and calculate time duration for the melting progression of the overall homogenous structure using Equation (7). An approach that is similar in concept to the approach conducted by [28] in their semi-analytical approach .

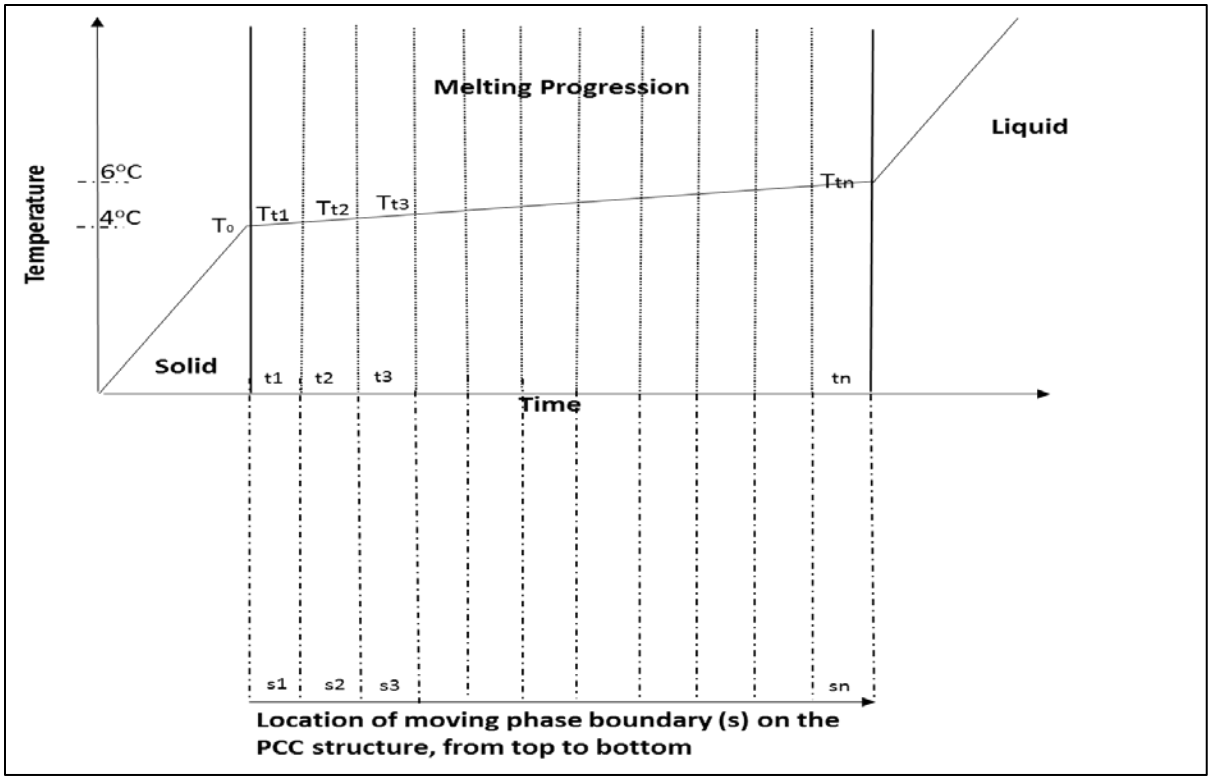

Figure 4: conceptual approach to calculate time duration with respect to temperature and position

Here are examples of the discretization of the model to calculate the time duration for the overall structure as illustrated by (Figure 4):

$$t1 = \frac{\Delta m * \Delta h \ * s^2}{2 * \lambda_{PCM} * (T_{t1} - T_{0})} \left(\frac{A_{PCM}}{A_{eff-tube}}\right)\left(1 + \frac{2 * \lambda_{PCM}}{s * k}\right) \quad (7a)$$

$$t2 = \frac{\Delta m * \Delta h \ * s^2}{2 * \lambda_{PCM} * (T_{t2} - T_{0})} \left(\frac{A_{PCM}}{A_{eff-tube}}\right)\left(1 + \frac{2 * \lambda_{PCM}}{s * k}\right) \quad (7b)$$

$$tn = \frac{\Delta m * \Delta h \ * s^2}{2 * \lambda_{PCM} * (T_{tn} - T_{0})} \left(\frac{A_{PCM}}{A_{eff-tube}}\right)\left(1 + \frac{2 * \lambda_{PCM}}{s * k}\right) \quad (7n)$$

5. Material Evaluation

Table 1 illustrates key components and properties of the PCC material that was used to build the model in Aspen Plus®.

Table 1: Phase change composite (PCC) material

Phase Change Composite (PCC)	
Composition	Paraffin + Graphite
Composition %	78% Paraffin + 22% Graphite
Energy Content	180 kJ/kg
Melting Range	4.0 -6.0 ^{0}C

Table 2 illustrates the properties of the AC's refrigerant (R-410A) and the properties of the heat transfer fluid (HTF), namely Ethylene Glycol (EG), being the intermediate loop.

Tabel 2: AC refrigerant loop data & ethylene glycol (EG) data

Air Conditioning's refrigerant		Intermediate loop (Ethylene Glycol)	
Type	R-410A	Type	Ethylene Glycol (EG)
Composition %	50% CH_2F_2 + 50% CHF_2CF_3	Composition %	50% EG + 50% Water

6. Model Validation

The simulation model developed for this research work was validated by crosschecking the simulation model's results with the results from an actual experimental system of 4 kWh PCC-TES benchtop thermal storage system. The actual 4 kWh PCC-TES benchtop system was built for actual testing and proof of concept purposes. Figure 5a shows a schematic of the main components of the overall PCC-TES system. Figure 5b illustrates the actual 4 kW PCC-TES benchtop system.

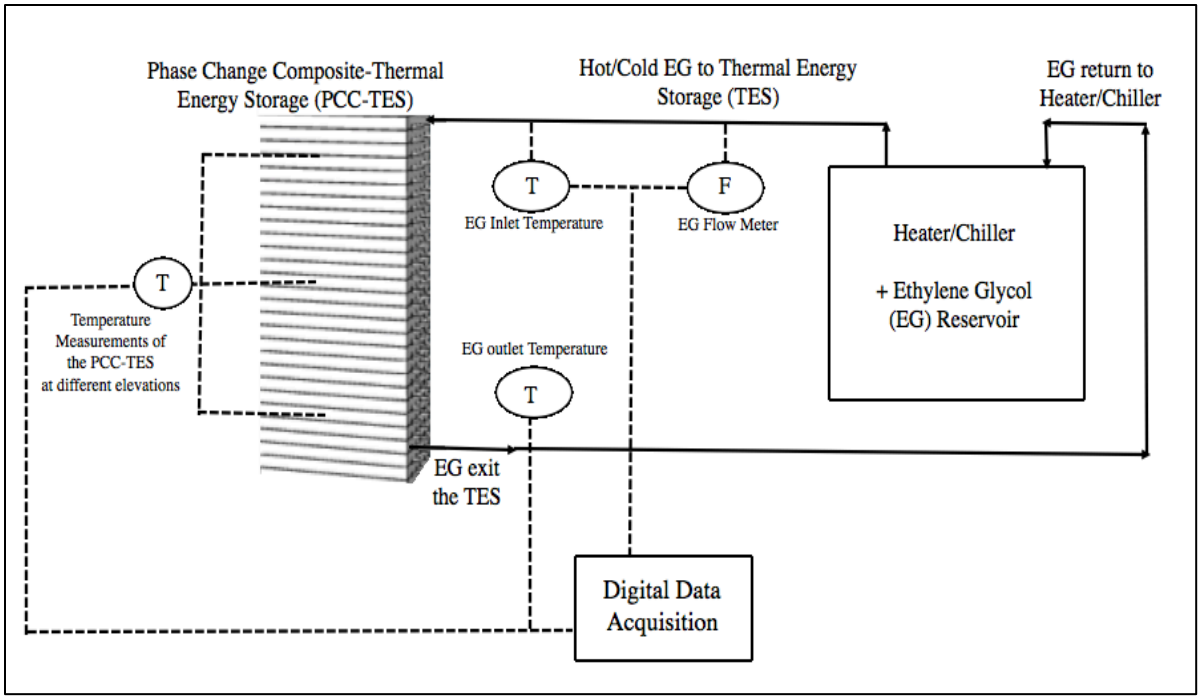

Figure 5a: Schematic of the PCC-TES system's main components

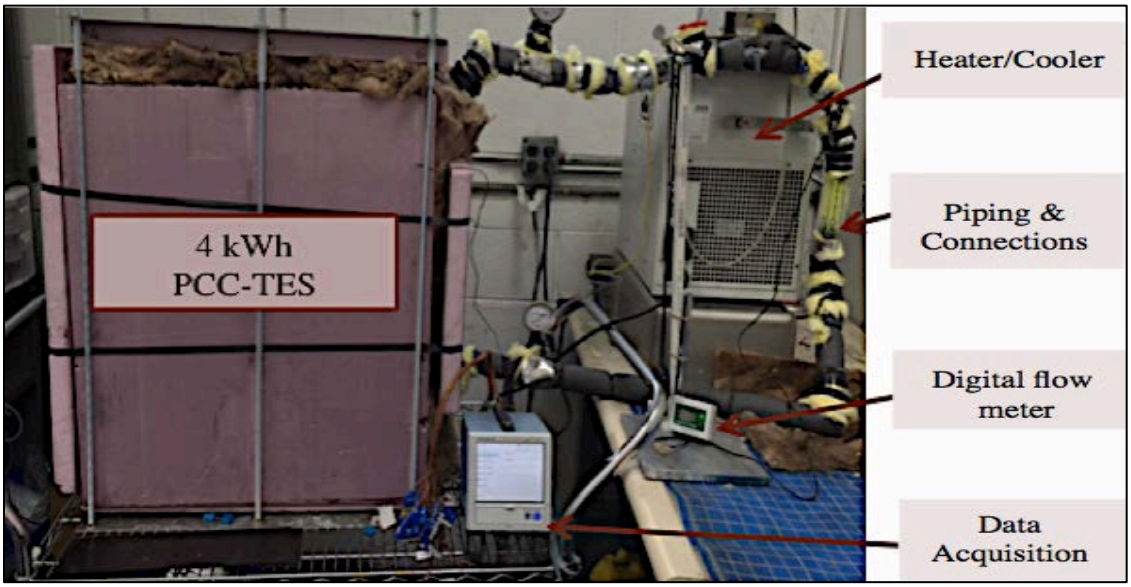

Figure 5b: Actual 4kWh PCC-TES system's main components

The first checkpoint was to verify if the developed Aspen Plus® simulation model enhanced with the required scientific equations and the heat transfer analytical model can adequately mimic the actual 4KWh PCC TES benchtop system's performance and anticipate equivalent results. Therefore, the evaluation model was

built reflecting the exact dimensions and storage capacity of the 4 kWh PCC-TES benchtop system. The simulation model also mimicked the flow rate and composition of the heat transfer fluid (HTF), namely ethylene glycol (EG). The specifications and dimensions of the real experimental setup and accordingly the model are illustrated in Table 3. As stated in the introduction section, this paper evaluates the feasibility of utilizing the proposed phase change composite (PCC) material to serve as the storage medium for a TES system for cooling applications. Therefore, it was a good starting point to check if the proposed PCC-TES can actually proof the concept and capabilities of storing and releasing thermal energy by exchanging heat with EG.

Table 3: Simulation model validation: (model input vs. real experiment input) for the actual 4 kWh PCC-TES benchtop

Real Experiment Data		**Input to Model's equations**	
PCC Latent Heat (kJ/kg)	180	PCC Latent Heat (KJ/Kg)	180
Slab Dimension: length, Width and thickness (m)	(0.46, 0.26 and 0.0254)	Slab Dimension: length, Width and thickness (m)	(0.46, 0.26 and 0.0254)
Number of Slabs (#)	28	Number of Slabs (#)	28
Total Mass of PCC slabs (kg)	78	Total Mass of PCC slabs (kg)	78
Weight (%) of paraffin and Graphite in each slab	(78% paraffin + (22% graphite)	Weight (%) of paraffin and Graphite in each slab	(78% paraffin + (22% graphite)
Copper tube outer diameter (in)	0.38	Copper tubes outer diameter (in)	0.38
Copper tube inner diameter (in)	0.32	Copper tubes inner diameter (in)	0.32
Total length of copper tube used	51 meters	Total length of copper tube used	51 meters
Ethylene Glycol volumetric flow rate (l/min)	2.3	Ethylene Glycol volumetric flow rate (l/min)	2.3
Ethylene Glycol input Temperature (C)	14	Ethylene Glycol input Temperature (C)	14
Solidified (cold) PCC initial temperature	-2	Solidified (cold) PCC initial temperature	-2
PCC melting range (^{0}C)	4-6	PCC melting range (^{0}C)	4-6

Air inlet temperature (^{0}C)	Not tested (heat exchange of EG and Air was not part of the actual testing	Air inlet temperature (^{0}C)	40

As illustrated by Figures 5a and 5b, the experimental setup is divided into three main components: (1) the actual 4 kWh PCC-TES system (2) the copper tubes (3) the chiller/heater. The first component is the actual 4 kWh PCC-TES consisting of graphite, which is the structure that holds the PCM and boosts thermal conductivity, and n-Tetradecane, which serves as the PCM that is capable of storing or releasing heat depending on the mode of operations; whether discharging or charging. The actual 4 kWh PCC-TES structure is made of 28 slabs of PCC. The whole PCC-TES structure is thermally insulated with building insulation materials. Each slab represents a graphite structure that has been soaked into n-Tetradecane for at least 24 hours until impregnated with n-Tetradecane. The slabs are numbered from top to bottom; top being number 1. The second component is the copper tubes or the copper coils, which pass back and forth in between the 28 slabs. The copper tubes enter the PCC-TES structure from the top and exits from the bottom of the structure. The EG stream runs through the copper tubes. The third component is the chiller/heater that is the device that controls the temperature of the EG being pumped through the tubes to exchange heat with the PCC-TES and also serves as the EG reservoir. Depending on whether it is intended to be a discharging or charging experiment, the chiller/heater set the temperature of the EG to (14) or (-2) ^{o}C, respectively. As introduced earlier, discharging mode takes place when the PCC-TES stores thermal energy and melts. On the other hand, during charging mode the PCC-TES rejects the stored heat to the cold EG passing through and solidifies. The discharging experiment was the chosen mode to be conducted and tracked in order to validate the simulation model. Therefore, the initial temperature of the 4 kWh PCC-TES system was set to (-2) ^{o}C marking a "completely solidified" PCC-TES status; after being charged (or solidified) using a cold EG stream in prior perpetration setups. For the discharging experiment, the EG fluid flow rate was set to 2.3 liter per minute. The initial temperature of the EG fluid was set to 14 ^{o}C by the chiller/heater controller. The official recorded starting time of the experiment was at the moment at which the 14 ^{o}C EG was pumped through cold PCC-TES. Few minutes later, the temperature of the EG existing the PCC-TES dropped down to 6 ^{o}C, rejecting the heat to the 4 kWh PCC-TES. The EG exiting the bottom of the PCC-TES was again rerouted through the outlet piping back to the chiller/heater to be heated again to 14 ^{o}C and back to the PCC-TES. The EG continued to leave the bottom of the PCC-TES at 6 ^{o}C until the PCC-TES approached "completely melted" status. Then, the temperature of the EG

exiting the bottom of the PCC-TES started to rise above 8 °C after a little over 3 hours of heat exchange. The discharging experiment was considered officially stopped at the moment at which the EG temperature reached 10 °C approximately after 3 hours and a half. Output parameters of the simulation model and actual discharging experiment are listed in Table 4.

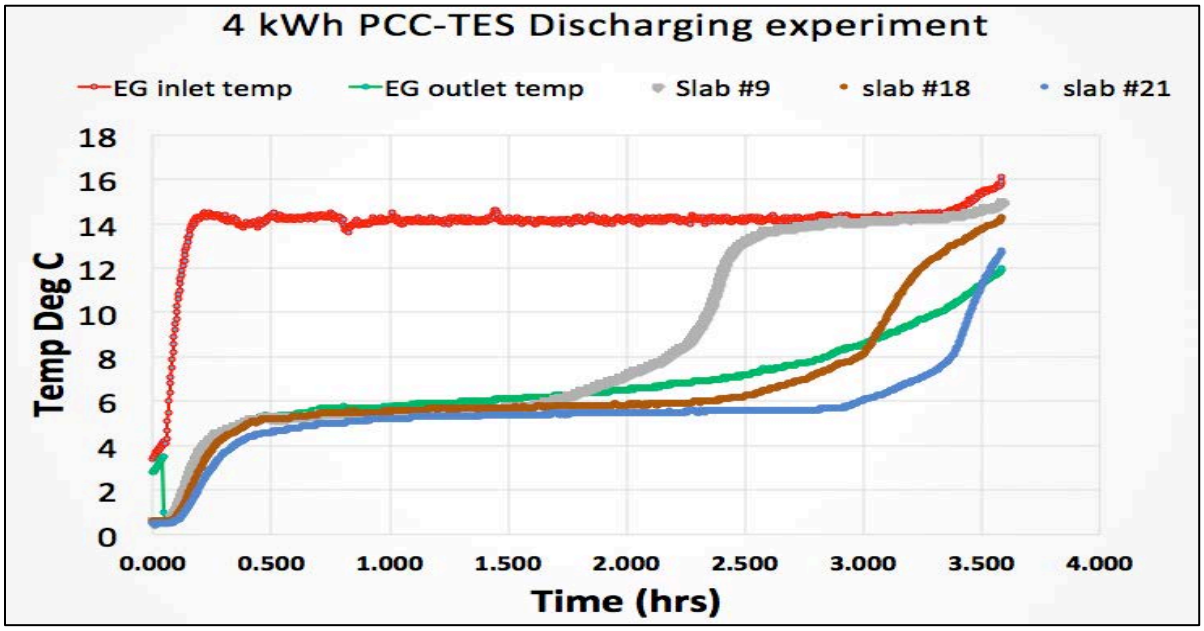

Figure 6: Representation of discharging experiment temperature profiles with respect to time

Figure 6 illustrates the temperature profiles of selected slabs during the discharging experiment. The EG inlet and outlet temperatures are indicated by the red and green curves, respectively. The temperature probe labeled (slab #9) on Figure 6 illustrates the temperature profile of the 9th slab of the actual PCC-TES, which is located at the top quarter of the PCC-TES structure. On the other hand, the temperature probe labeled (slab #12) represents the temperature of the 12th slab located on 2nd quarter segment of the PCC-TES. As indicates, slab number 9 melted before slab number 18 because the hot EG enters the PCC-TES at the top and leaves out at the bottom. Likewise, slab number 18 melted before slab number 21. This illustrates a top to bottom melting profile of the slabs, which is a rational consequence to the fact that hot EG enters the PCC-TES from the top and leaves of the bottom. Duration of useful heat exchange revealed by the actual experiment was approximately 3 hours and 27 minutes. The actual experiment duration also accounted for sensible heat before and after melting in addition to melting duration.

Table 4: Simulation model validation: (model output vs. experimental results) for the actual 4 KWh PCC-TES benchtop

Real Experiment Data		Model Output	
Discharging rates (time)	3 hours and 27 minutes	Discharging rates (time)	3 hours and 37 minutes
Time frame	(Sensible heat before melting + melting duration + Sensible heat after	Time frame	(Sensible heat before melting + melting duration + Sensible heat after melting)
EG outlet temperature (^{0}C)	6	EG outlet temperature (^{0}C)	6
PCC final temperature (^{0}C)	10	PCC final temperature	10
Air outlet temperature (^{0}C)	Not tested (heat exchange of EG and Air was not part of the actual testing setup, only in modeling part)	Air outlet temperature (^{0}C)	18
Air volumetric flow rate (CFM)	Not tested (heat exchange of EG and Air was not part of the actual testing setup, only in modeling part)	Air volumetric flow rate (CFM)	370

On the other hand, as illustrated by Table 4, the simulation model anticipated the whole PCC-TES structure to fully discharge in approximately 3 hours and 37 minutes, providing 4 kW of useful heat. The small discrepancy in discharging duration is attributed to possible heat loss to surroundings in the actual experiment.

In light of the very good agreements between the experimental data and the evaluation model's forecast, the simulation model was considered validated and was ready to perform further analysis. On final remark and prior to proceed with further analysis, it is worth mentioning that one of the main advantages of simulation modeling over actual experimental testing is the capability of simulating downstream heat exchange between EG intermediate loop and the air stream while that was not a provision in the actual experimental setup. One more advantage of simulation modeling over actual testing is the capability of changing dimensions, thermal capacities and operating strategies without having to build multiple actual experimental setups.

7. Case study

In previous sections, the concept of integrating a TES with phase change material into an AC system was introduced. In addition to that, simulation model's scientific background, developmental approach and model validation were also discussed. This

section will utilize the validated simulation model to evaluate and analyze the following conceptual case study.

7.1 Case study: AC integrated with PCC-TES vs. Conventional AC without a TES

This case study explores whether or not the concept of integrating a PCC-TES (Phase Change Composite-Thermal Energy Storage) into an AC system can have a positive impact on the overall air conditioning system performance and electricity consumption. The validated simulation model was used to address the performance comparison.

7.1.1 Comparison criteria

To conduct the case study, two air conditioning systems were simulated, analyzed and compared: (1) a conventional AC without a TES (2) a conventional AC integrated with a PCC-TES were. The comparison analysis was performed with respect to the following criteria: refrigeration compressor size (kW), electricity consumed (kWh) by the compressor, cost of electricity consumed by the compressor ($), compressor efficiency during cooler hours/days of the year and CO_2 emissions (lbs. of CO_2).

7.1.2 Testing basis

As far as the price of electricity consumed by the compressor, this present work applied Southern California Edison Electric utility company (ToU) rate plan on year 2016 [5]. That is 0.235 $/kWh from 12 pm to 6 pm plus a demand charge of $9.5/MAX kW for each billing cycle. The company applies $0.191/kWh and $0.064/kWh electricity ToU charges for mid-peak and off-peak hours, respectively. As illustrated by Table 5, both systems were required to meet the same thermal cooling loads of 16 kW and 8 kW during peak hours and mid peak hours, respectively. No cooling loads were required to be met during off-peak hours assuming a small shop space or a restaurant that closes during that time.

Table 5: Cooling load demand required to be met by both systems

Cooling Load Required to be met by both systems	
Peak hours (noon- 6 pm)	16 kW
Mid Peak hours during: (9 am- Noon) & (6 pm -11pm)	8 kW
Off-Peak hours (11pm-9am)	No Requirement

7.1.3 Results and discussion

Following the preliminary design stage for the refrigeration cycle for each of the two systems using the developed and validated Aspen Plus® simulation model, the following facts were revealed:

1) 5 kW Compressor is required for the "conventional AC with no TES" to meet the 16 kW per hour of thermal cooling load during each of the six peak hours. However, it is oversized for the 8 kW per hour thermal cooling demand during each of the mid peak hours.
2) 2.5 kW compressor is required for the new proposed system (AC + PCC-TES) to meet 50% of the 16 kW thermal cooling load requirement during each hour of the six peak hours while the PCC-TES meets the other half of cooling load requirement. During mid peak hours, the 2.5 kW compressor has just the precise size needed to meet the cooling demand.
3) The other half of the thermal cooling load during each of the six peak hours will be met the by PCC-TES. Accordingly, a total of 960 kg of PCC is required to meet the cooling load demand of 8 kW that is equivalent to 28,800 kJ on each of the six peak hours, a total of 172,800 kJ during the whole 6-hour- peak period. On each peak hour, approximately 160 kg of PCC will be melted; recall that PCC has latent heat of 180 kJ/kg.

Table 6 summarized the overall results of the case study's performance comparison. As illustrated by Table 6, integrating a conventional AC with a PCC-TES would result in designing for a smaller refrigerant loop and accordingly a smaller compressor size. The smaller compressor is also just the right size for mid/off-peak hours. The new compressor is neither oversized for cooler mid/off-peak hours nor oversized for the other cooler seasons of the year. The Aspen Plus® simulation model showed that the proposed system (AC + PCC-TES) would have the advantage of 50% approximate reduction in refrigerant compressor size. Running a 50% smaller compressor during cooler hours/days of the year, instead of an oversized compressor, will reduce electricity consumed and CO_2 emissions. Due to smaller refrigerant compressor, proposed system would result in 45% reduction in electricity bill. Similarly, proposed integration of (AC + PCC-TES) would result in approximately 30% reduction in CO_2 emissions during a summer season in comparison to conventional AC's CO_2 emissions. Moreover, proposed integration would result in doubling the COP (Coefficient of Performance) during mid and off-peak hours in comparison to the COP of an oversized conventional AC during those hours. The COP is doubled during mid/off-peak hours because of the fact that the new AC (integrated with the PCC-TES) is not oversized anymore to meet the peak hours of a summer season, it is now just the right size for mid/off-peak hours demand. A conventional AC without a TES is usually designed to be large enough to handle summer seasons, yet oversized for other seasons. Therefore, this case study concluded that integrating a conventional AC with

a PCC-TES would certainly have great positive impacts on the overall system performance and electricity consumption as demonstrated by Table 6.

Table 6: Modeling Comparison: Conventional AC vs. an integrated unit (AC+ PCC-TES)

Details	Conventional AC	Integrated unit (AC + PCC-TES)	Quantified Benefits of integrated system (AC + PCC-TES)
Compressor Size + Storage Size	5 kW + no storage	2.5 kW + 960 KG of PCC thermal storage	50% reduction in compressor size
COP (During Mid/off-peak)	1.6	3.2	Double COP during Mid/Off-peak hours
Electricity consumed by the refrigeration compressor (kWh/Summer)	4,200 kWh	3,000 kWh	Approximately 30% reduction in electricity consumption during a
Cost of Electricity Consumption ($)	$ 929	$ 522	45% reduction in electricity bill during a summer season
CO_2 Emission (lb. CO_2/Summer Season)	2,200 lbs. CO_2	1,572 lbs. CO_2	Approximately 30% reduction in CO_2 emissions during a summer season

The analysis in this case study revealed that integrating a conventional AC with a PCC-TES would certainly have positive impacts on the overall conditioning system performance and electricity consumption. The proposed integration would result in 50% smaller AC's compressor design requirement, 30% lower electricity consumption, 45% lower electricity bill and 30% lower CO_2 emissions during expensive peak hours of a summer season.

8. Conclusions

The work of this paper successfully tested and verified the proposed hypothesis, which suggests that integrating a conventional AC with a PCC-TES, would result in great benefits concerning compressor size, compressor efficiency, electricity consumption and CO_2 emissions. The subject integration would contribute to completely or partially shift electricity demand from peak hours to off-peak hours; contributing to reduce the worldwide ever-increasing electricity demand during peak hours. This would contribute to reduce necessity for building additional expensive new power plants and distribution infrastructure. To test the hypothesis, a simulation model in Aspen Plus® software was prepared. However, Aspen Plus® did not have an

in-built library to predict PCC's melting and solidification behaviors. Therefore, an analytical heat transfer model was written as a system of equations in Fortran into Aspen Plus® calculation block to simulate the phase change behavior and associated valuable information. The simulation of the proposed integration between the AC and the PCC-TES revealed that the proposed integration would result in downsizing compressor design by 50%, lowering electricity consumption by 30%, doubling the efficiency during mid and off-peak hours, and lowering CO_2 emissions by 30%. The simulation model was validated by crosschecking the simulation model results with actual experimental data from an actual 4 kWh PCC-TES benchtop thermal storage system. A very good agreement between the simulation model results and the actual experimental data was observed. The present work is a conceptual design and optimization study and does not account for integration inefficiencies, energy losses, real-world operation complexity, and added capital cost of TES integration with AC systems. Such issues will be addressed in future publications.

Acknowledgements

The authors acknowledge the valuable contributions and access to R&D facilities by our industry partners AllCell Technologies LLC, and NETenergy.

Work cited

1. Ubay BJ. Air conditioning. Ocean Engineering.
2. Rhodes JD, Stephens B, Webber ME. Using energy audits to investigate the impacts of common air-conditioning design and installation issues on peak power demand and energy consumption in Austin, Texas. *Energy Build*. 2011;43(11):3271-3278. doi:10.1016/j.enbuild.2011.08.032
3. Izquierdo M, Moreno-Rodríguez A, González-Gil A, García-Hernando N. Air conditioning in the region of Madrid, Spain: An approach to electricity consumption, economics and CO2 emissions. *Energy*. 2011;36(3):1630-1639. doi:10.1016/j.energy.2010.12.068
4. Lahn G, Stevens P. Burning Oil to Keep Cool: the Hidden Energy Crisis in Saudi Arabia. The Royal Institute of International Affairs. http://www.chathamhouse.org/sites/files/chathamhouse/public/Research/Energy, Environment and Development/1211pr_lahn_stevens.pdf. Published 2011.
5. Southern California Edison. Tariffs and programs for small, medium, and large power customers, plan GS-2 Time of Use (TOU) rate "option A", 2016. 2016.
6. Farid MM, Khudhair AM, Razack SAK, Al-Hallaj S. A review on phase change energy storage: Materials and applications. *Energy Convers Manag*. 2004;45(9-

10):1597-1615. doi:10.1016/j.enconman.2003.09.015
7. Bo H, Gustafsson EM, Setterwall F. Tetradecane and hexadecane binary mixtures as phase change materials (PCMs) for cool storage in district cooling systems. *Energy*. 1999;24(12):1015-1028. doi:10.1016/S0360-5442(99)00055-9
8. Arteconi A, Hewitt NJ, Polonara F. State of the art of thermal storage for demand-side management. *Appl Energy*. 2012;93:371-389. doi:10.1016/j.apenergy.2011.12.045
9. MacPhee D, Dincer I. Performance assessment of some ice TES systems. *Int J Therm Sci*. 2009;48(12):2288-2299. doi:10.1016/j.ijthermalsci.2009.03.012
10. Henze GP, Biffar B, Kohn D, Becker MP. Optimal design and operation of a thermal storage system for a chilled water plant serving pharmaceutical buildings. *Energy Build*. 2008;40(6):1004-1019. doi:10.1016/j.enbuild.2007.08.006
11. Yau YH, Rismanchi B. A review on cool thermal storage technologies and operating strategies. *Renew Sustain Energy Rev*. 2012;16(1):787-797. doi:10.1016/j.rser.2011.09.004
12. Hasnain SM. Review on sustainable thermal energy storage technologies, Part II: cool thermal storage. *Energy Convers Manag*. 1998;39(11):1139-1153. doi:10.1016/S0196-8904(98)00024-7
13. Zhai XQ, Wang XL, Wang T, Wang RZ. A review on phase change cold storage in air-conditioning system: Materials and applications. *Renew Sustain Energy Rev*. 2013;22:108-120. doi:10.1016/j.rser.2013.02.013
14. He B, Setterwall F. Technical grade paraffin waxes as phase change materials for cool thermal storage and cool storage systems capital cost estimation. *Energy Convers Manag*. 2002;43(13):1709-1723. doi:10.1016/S0196-8904(01)00005-X
15. Arasu A valan, Sasmito AP, Mujumdar AS. Numerical performance study of paraffin wax dispersed with alumina in a concentric pipe latent heat storage system. *Therm Sci*. 2013;17(2):419-430. doi:10.2298/TSCI110417004A
16. Mills A, Farid M, Selman JR, Al-Hallaj S. Thermal conductivity enhancement of phase change materials using a graphite matrix. *Appl Therm Eng*. 2006;26(14-15):1652-1661. doi:10.1016/j.applthermaleng.2005.11.022
17. Sarler B. Stefan â€™ s work on solid-liquid phase changes. 1995;7997(95):83-92.
18. Vuik C. Some historical notes on the Stefan problem . The Stefan problem . The Stefan problem with a linear temperature profile . 1984:1-10.
19. Font F. *Beyond the Classical Stefan Problem*.; 2014.
20. Voller V, Cross M. Accurate solution of moving boundary problems using the enthalpy method. *Int J Heat Mass Transf*. 1981;24:545-556.
21. Kostenko BF, Pribis J, Puzynin I V. Stefan's problem and beyond. *arXiv*. 2003:1-13. http://arxiv.org/abs/math-ph/0302044.
22. Khateeb SA, Amiruddin S, Farid M, Selman JR, Al-Hallaj S. Thermal

management of Li-ion battery with phase change material for electric scooters: Experimental validation. *J Power Sources*. 2005;142(1-2):345-353. doi:10.1016/j.jpowsour.2004.09.033

23. Sharma A, Tyagi V V., Chen CR, Buddhi D. Review on thermal energy storage with phase change materials and applications. *Renew Sustain Energy Rev*. 2009;13(2):318-345. doi:10.1016/j.rser.2007.10.005
24. Iten M, Liu S. A work procedure of utilising PCMs as thermal storage systems based on air-TES systems. *Energy Convers Manag*. 2014;77:608-627. doi:10.1016/j.enconman.2013.10.012
25. Mehling, Harald and LFC. *Heat and Cold Storage with PCM: An up to Date Introduction into Basics and Applications.* Berlin: Springer; 2008.
26. Hans Dieter Baehr and Karl Stephan. *Heat and Mass Transfer*. 2nd, revis ed. Berlin: Springer; 2014.
27. Wu S, Fang G, Chen Z. Discharging characteristics modeling of cool thermal energy storage system with coil pipes using n-tetradecane as phase change material. *Appl Therm Eng*. 2012;37:336-343. doi:10.1016/j.applthermaleng.2011.11.046
28. P. Dolado, A. Lázaro, B. Zalba JMMT. Numerical Simulation of the Thermal Behaviour of an Energy Storage Unit With Phase Change Materials for Air Conditioning Applications Between 17°c and 40°c. *Proc Tenth Int Conf Therm Energy Storage, Ecostock 2006*. 2006.